LEARNING PREDICTIVE CHECKLISTS WITH PROBABILISTIC LOGIC PROGRAMMING

Anonymous authors
Paper under double-blind review

ABSTRACT

Checklists have been widely recognized as effective tools for completing complex tasks in a systematic manner. Although originally intended for use in procedural tasks, their interpretability and ease of use have led to their adoption for predictive tasks as well, including in clinical settings. However, designing checklists can be challenging, often requiring expert knowledge and manual rule design based on available data. Recent work has attempted to address this issue by using machine learning to automatically generate predictive checklists from data, although these approaches have been limited to Boolean data. We propose a novel method for learning predictive checklists from diverse data modalities, such as images and time series, by combining the power of dedicated deep learning architectures with the interpretability and conciseness of checklists. Our approach relies on probabilistic logic programming, a learning paradigm that enables matching the discrete nature of checklist with continuous-valued data. We propose a regularization technique to tradeoff between the information captured in discrete concepts of continuous data and permit a tunable level of interpretability for the learned checklist concepts. We demonstrate that our method outperforms various explainable machine learning techniques on prediction tasks involving image sequences, medical time series, and clinical notes.

1 INTRODUCTION

In recent years, machine learning models have gained popularity in the healthcare domain due to their impressive performance in various medical tasks, including diagnosis from medical images and early prediction of sepsis from clinical time series, among others (Davenport & Kalakota, 2019; Esteva et al., 2019). Despite the proliferation of these models in the literature, their wide adoption in real-world clinical practice remains challenging (Futoma et al., 2020; Ahmad et al., 2018; Ghassemi et al., 2020; De Brouwer et al., 2022). Ensuring the level of robustness required for healthcare applications is difficult for deep learning models due to their inherent black box nature. Non-interpretable models make stress testing arduous and thus undermine the confidence required to deploy them in critical applications such as clinical practice. To address this issue, recent works have focused on developing novel architectures that are both human-interpretable and retain the high performance of black box models (Ahmad et al., 2018).

One such approach is learning medical checklists from available medical records. Due to their simplicity and ability to assist clinicians in complex situations, checklists have become increasingly popular in medical practice (Haynes et al., 2009). However, the simplicity of using checklists typically contrasts with the complexity of their design. Creating a performant checklist requires domain experts who manually collect evidence about the particular clinical problem of interest (Hales et al., 2008), and subsequently reach consensus on meaningful checklist rules (Hales et al., 2008). As the number of available medical records grows, the manual collection of evidence becomes more tedious, bringing the need for partially automated design of medical checklists.

Recent works have taken a step in that direction by learning predictive checklists from Boolean, categorical, or continuous tabular data (Zhang et al., 2021; Makhija et al., 2022). Nevertheless, many available clinical data, such as images or time series, are nor categorical nor tabular by nature. They therefore fall outside the limits of applicability of previous approaches for learning checklists from data. This work aims at addressing this limitations.

Prior work leverages integer programming to generate checklists, but the discrete (combinatorial) nature of solving integer programs makes it challenging to learn predictive checklists from images or time series data. Deep learning architectures rely on gradient-based optimization which differs in style and is difficult to reconcile with integer programming (Shvo et al., 2021). We instead propose to formulate predictive checklists within the framework of probabilistic logic programming. This enables us to extract binary concepts from high-dimensional modalities like images, time series, and text data according to a probabilistic checklist objective, while propagating derivatives throughout the entire neural network architecture. Unlike existing approaches, ProbChecklist doesn't rely on fixed summary extractors such as mean or standard deviation of time series; instead, it learns concepts using neural networks (concept learners).

Our architecture, ProbChecklist, operates by creating binary concepts from high-dimensional inputs, which are then used for evaluating the checklist. However, they are learnt with deep neural networks and are not necessarily interpretable. We therefore investigate two different strategies for providing predictive yet interpretable concepts. The first relies on using inherently interpretable concept extractors, which only focus on specific aspects of the input data (Johnson et al., 2022). The second adds regularization penalties to enforce interpretability in the neural network by design. Several regularization terms have been coined to ensure the concepts are unique, generalizable, and correspond to distinctive input features (Jeffares et al., 2023) (Zhang et al., 2018).

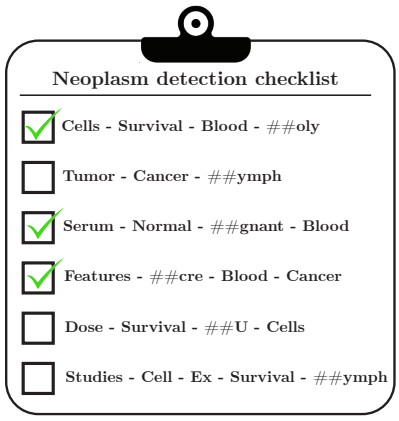

Figure 1: Example checklist learnt by our architecture. Three or more checks entail a positive neoplasm prediction.

Clinical practice is a highly stressful environment where complex decisions with far-reaching consequences have to be made quickly. In this context, the simplicity, robustness, and effectiveness of checklists can make a difference (Hales et al., 2007). Healthcare datasets contain sensitive patient information, including ethnicity and gender, which should not cause substantial differences in the treatment provided. Nevertheless, machine learning models trained on clinical data have been shown to exhibit unacceptable imbalance of performance for different population groups, resulting in biased predictions. When allocating scarce medical resources, fairness should be emphasized more than accuracy to avoid targeting minority subgroups (Fawzy et al., 2022). In an attempt to mitigate this problem, we study the impact of including a fairness regularization into our architecture and report significant reductions in the performance gap across sensitive populations.

We validate our approach empirically on several classification tasks using various data modalities such as images and clinical time series. We show that ProbChecklist outperforms previous learnable predictive checklist approaches as well as several interpretable machine learning baselines. We showcase the capabilities of our method on two healthcare case studies, learning interpretable checklists to early predict the occurrence of sepsis and mortality prediction for intensive care patients.

Contributions.

- We propose the first framework to learn predictive checklists from arbitrary input data modalities. Our approach can learn checklists and extract meaningful concepts from time series and images, among others. In contrast with previous works that used (mixed-)integer programming, our approach formulates the predictive checklist learning within the framework of probabilistic logical programming.
- We investigate the impact of different schemes for improving the interpretability of the concepts learnt as the basis of the checklist. We employ regularization techniques to encourage the concepts to be distinct, so they can span the entire input vector and be specialized, i.e. ignore the noise in the signal and learn sparse representations. We also investigate the impact of incorporating fairness constraints into our architecture.
- We validate our learning framework on different data modalities such as images, text and clinical time series, displaying significantly improved performance compared to state-of-the-art checklist learning schemes.

2 RELATED WORKS

A major motivation for our work is the ability to learn effective yet interpretable predictive models from data, as exemplified by the interpretable machine learning literature. Conceptually, our method builds upon the recent body of work on learning predictive checklists from data. The implementation of our solution is directly inspired by the literature on probabilistic logic programming.

Interpretable machine learning. Motivated by the lack of robustness and trust of black box models, a significant effort has been dedicated to developing more human-interpretable machine learning models in the last years (Ahmad et al., 2018; Murdoch et al., 2019). Among them, one distinguishes between *intrinsic* (*i.e.* when the model is itself interpretable such as decision trees) and *posthoc* (*i.e.* when trained models are interpreted a posteriori) methods (Du et al., 2019). Checklists belong to the former category as they are an intuitive and easy to use decision support tool. Compared to decision trees, checklists are more concise (there is no branching structure) and can thus be potentially more effective in high stress environments (a more detailed argument is presented in Appendix D). Our approach also relies on building concepts from the input data. Because the concepts are learnt from data, they may themselves lack a clear interpretation. Both intrinsic and posthoc interpretability techniques can then be applied for the concept extraction pipeline (Jeffares et al., 2023). Concept Bottleneck Models (Koh et al., 2020) insert a concept layer before the last fully connected layer, assigning a human-understandable concepts to each neuron. However, a major limitation is that it requires expensive annotated data for predefined concepts.

Rule-based learning. Boolean rule mining and decision rule set learning is a well-studied area that has garnered considerable attention spurred by the demand for interpretable models. Some examples of logic-based models include Disjunctive Normal Forms (OR of ANDs), Conjunctive Normal Forms (AND of ORs), chaining of rules in the form of IF-THEN-ELSE conditions in decision lists, and decision tables. Most approaches perform pre-mining of candidate rules and sample rules using integer programs (IP), simulated annealing, performing local search algorithm for optimizing simplicity and accuracy (Lakkaraju et al., 2016), and Bayesian framework for constructing a maximum a posteriori (MAP) solution (Wang et al., 2017).

Checklist learning. Checklists, pivotal in clinical decision-making, are typically manually designed by expert clinicians (Haynes et al., 2009). Increasing medical records make manual evidence collection tedious, prompting the need for automated medical checklist design. Recent works have taken a step in that direction by learning predictive checklists from Boolean or categorical medical data (Zhang et al., 2021). Makhija et al. (2022) have extended this approach by allowing for continuous tabular data using mixed integer programming. Our work builds upon these recent advances but allows for complex input data modalities. What is more, in contrast to previous works, our method does not rely on integer programming and thus exhibits much faster computing times and is more amenable to the most recent deep learning stochastic optimization schemes.

Probabilistic logical programming. Probabilistic logic reasoning combines logic and probability theory. It represents a refreshing framework from deep learning in the path towards artificial intelligence, focusing on high-level reasoning. Examples of areas relying on these premises include statistical artificial intelligence (Raedt et al., 2016; Koller et al., 2007) and probabilistic logic programming (De Raedt & Kimmig, 2015). More recently, researchers have proposed hybrid architectures, embedding both deep learning and logical reasoning components (Santoro et al., 2017; Rocktäschel & Riedel, 2017; Manhaeve et al., 2018). Probabilistic logic reasoning has been identified as important component for explainable or interpretable machine learning, due to its ability to incorporate knowledge graphs (Arrieta et al., 2020). Combination of deep learning and logic reasoning programming have been implemented in interpretable computer vision tasks, among others (Bennetot et al., 2019; Oldenhof et al., 2023).

3 BACKGROUND

Problem Statement: We consider a supervised learning problem where we have access to N input data points $\mathbf{x}_i \in \mathcal{X}$ and corresponding binary labels $y_i \in \{0, 1\}$. Each input data point consists of a collection of K data modalities: $\mathbf{x}_i = \{\mathbf{x}_i^1, \mathbf{x}_i^2, \ldots, \mathbf{x}_i^K\}$. Each data modality can either be continuous ($\mathbf{x}_i^k \in \mathbb{R}^{d_k}$) or binary ($\mathbf{x}_i^k \in \{0, 1\}^{d_k}$). Categorical data are assumed to be represented in expanded binary format. We set d as the overall dimension of $\mathbf{x}_i$. That is, $d = \sum_{k=1}^{K} d_k$. The N input data points and labels are aggregated in a data structure $\mathbf{X}$ and a vector $\mathbf{y}$ respectively.

Our objective is to learn an interpretable decision function $f : \mathcal{X} \rightarrow \{0, 1\}$ from some domain $\mathbb{F}$ that minimizes some error criterion d between the predicted and the true label. The optimal function f^* then is: $f^* = \arg\min_{f \in \mathcal{F}} \mathbb{E}_{\mathbf{x},\mathbf{y} \sim \mathcal{D}}[d(f(\mathbf{x}), \mathbf{y})]$, where $\mathcal{D}$ stands for the observational data distribution. We limit the search space of decision functions $\mathcal{F}$ to the set of predictive checklists, which are defined below.

Predictive checklists: Generally, we define a predictive checklist as a linear classifier applying on a list of M binary concepts $\mathbf{c}_i \in \{0, 1\}^M$. A checklist will predict a data point, consisting of M concepts $\mathbf{c}_i = \{c_i^1, \ldots, c_i^M\}$, as positive if the number of concepts such that $c_i^m = 1$ is larger or equal to a threshold T. That is, given a data point with concepts $\mathbf{c}_i$, the predicted label of a checklist with threshold T is expressed as: $\hat{y}_i = \begin{cases} 1 & \text{if} \quad \sum_{m=1}^{M} c_i^m \geq T \\ 0 & \text{otherwise} \end{cases}$

The only parameter of a checklist is the threshold T. Nevertheless, the complexity lies in the definition of the list of concepts that will be given as input to the checklist. This step can be defined as mapping ϕ that produces the binary concepts from the input data: $\mathbf{c}_i = \psi(\mathbf{x}_i)$. Existing approaches for learning checklists from data differ by their mapping ψ. Zhang et al. (2021) assume that the input data is already binary. In this case, the mapping ψ_M is then a binary matrix $\Psi \in \{0, 1\}^{M \times k}$ such that $\Psi \mathbf{1}_k = \mathbf{1}_k$, where $\mathbf{1}_k$ is a column vector of ones[1]. One then computes $\mathbf{c}_i$ as $\mathbf{c}_i = \Psi_M \mathbf{x}_i$. The element of Ψ_M as well as the number of concepts M (hence the dimension of the matrix) are learnable parameters.

Previous approaches (Makhija et al., 2022) relax the binary input data assumption by allowing for the creation of binary concepts from continuous data through thresholding. Writing $\mathbf{x}_i^b$ and $\mathbf{x}_i^c$ for the binary and real parts of the input data respectively, the concept creation mechanism transforms the real data to binary with thresholding and then uses the same matrix Ψ_M. We have $\mathbf{c}_i = \Psi_M[\mathbf{x}_i^b, \text{sign}(\mathbf{x}_i^b - \mathbf{t}_i)]$, where $[\cdot, \cdot]$ is the concatenation operator, $\mathbf{t}_i$ is a vector of thresholds, $\text{sign}(\cdot)$ is an element-wise function that returns 1 is the element is positive and 0 otherwise. In this formulation one learns the number of concepts M, the binary matrix Φ_M as well as the thresholds values $\mathbf{t}_i$.

Probabilistic Logic Programming:

Probabilistic logical reasoning is a knowledge representation approach that involves the use of probabilities to encode uncertainty in knowledge. This is encoded in a probabilistic logical program (PLP) $\mathcal{P}$ connected by a set of N probabilistic facts $U = \{U_1, ..., U_N\}$ and M logical rules $F = \{f_1, ...f_M\}$. PLP enables inference on knowledge graphs $\mathcal{P}$ by calculating the probability of a query. This query is executed by summing over the probabilities of different "worlds" $w = u_1, ..., u_N$ (i.e., individual realizations of the set of probabilistic facts) that are compatible with the query q. The probability of a query q in a program $\mathcal{P}$ can be inferred as $P_{\mathcal{P}}(q) = \sum_w P(w) \cdot \mathbb{I}[F(w) \equiv q]$, where $F(w) \equiv q$ indicates that the propagation of the realization w across the knowledge graph, according to the logical rules F, leads to q being true. The motivation behind using PLP is to navigate the tradeoff between discrete checklists and learnable soft concepts. Incorporating a neural network into this framework enables the generation of probabilistic facts denoted as the neural predicate U^θ, where θ represents the weights. These weights can be trained to minimize a loss that depends on the probability of a query q: $\hat{\theta} = \arg\min_\theta \mathcal{L}(P(q \mid \theta))$.

4 PROBCHECKLIST: LEARNING FAIR AND INTERPRETABLE PREDICTIVE CHECKLISTS

4.1 ARCHITECTURE OVERVIEW

Our method first applies concept extractors on each data modality. Each concept extractor outputs a list of concept probabilities for each data modality. These probabilities are then concatenated to form a vector of probabilistic concepts ($\mathbf{p_i}$) for a given data sample. This vector is dispatched to a probabilistic logic module that implements a probabilistic checklist with query $q := \mathcal{P}(\mathbf{y_i} = \hat{\mathbf{y}}_\mathbf{i})$. We can then compute the probability of the label of each data sample and backpropagate through the whole architecture. At inference time, the checklist inference engines discretize the probabilistic

[1]This corresponds effectively to every row of Ψ summing to 1.

checklist to provide a complete predictive checklist. A graphical depiction of the overall architecture is given in Figure 2.

4.2 Data Modalities and Concepts

Data modalities refer to the distinct sets of data that characterize specific facets of a given process. For instance, in the context of healthcare, a patient profile typically includes different clinical time series, FMRI and CT-scan images, as well as prescriptions and treatment details in text format. The division in data modalities is not rigid but reflects some underlying expert knowledge. Concepts are characteristic binary variables that are learnt separately for each modality.

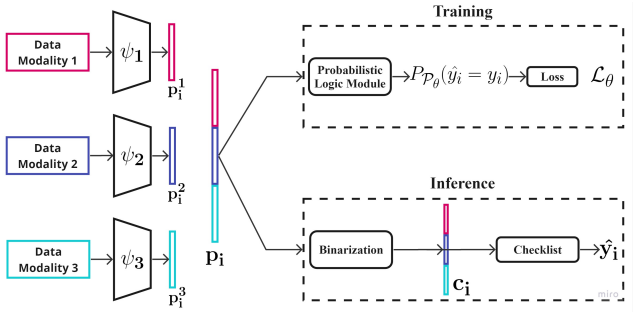

Figure 2: **Overview of our proposed ProbChecklist.** Given K data modalities as the input for sample i, we train K concept learners to obtain the vector of probabilistic concepts of each modality $\mathbf{p_i^k} \in [0,1]^{d'_k}$. Next, we concatenate into the full concepts probabilities ($\mathbf{p_i}$) for sample i. For training the concept learners, we pass $\mathbf{p_i}$ through the probabilistic logic module. At inference time, we discretize $\mathbf{p_i}$ to construct a complete predictive checklist.

4.3 Concept Extractor

Instead of directly learning binary concepts, we extract soft concepts that we subsequently discretize. For each of the K data modalities, we have a soft concept extractor $\psi_k : \mathbb{R}^{d_k} \to [0,1]^{d'_k}$ that maps the input data to a vector of probabilities $\mathbf{p}_i^k$, where d'_k is the number of soft concepts to be extracted from data modality k. Concatenating the outputs of the K concept extractors results in a vector of probabilities $\mathbf{p}_i \in [0,1]^{d'}$, with the d' the total number of soft concepts.

4.4 Checklist Learning

The checklist prediction formula of Equation 3 can be understood as logical rules in a probabilistic logical program. Together with the probabilities of each concepts, encoded in vector $\mathbf{p}_i$ that represent d' probabilistic facts, this represents a probabilistic logical program $\mathcal{P}_\theta$. We refer to θ as the set of learnable parameters in the probabilistic logical program.

We want to maximize the probability of a the prediction being correct. That is, we want to maximize the probability of the query $q := \hat{y}_i = y_i$,

$$\hat{\theta} = \arg\min_\theta -P_{\mathcal{P}_\theta}(\hat{y}_i = y_i) = \arg\min_\theta -\sum_w P(w) \cdot \mathbb{I}[F(w) \equiv (\hat{y}_i = y_i)] \tag{1}$$

By interpreting the probabilities $\mathbf{p}_i$ as the probability that the corresponding binary concepts are equal to 1 (*i.e.* $\mathbf{p}_i[j] = P(\mathbf{c}_i[j] = 1)$, where $[j]$ indexes the j-th component of the vector), we can write the probability of query q as follows.

Proposition 4.1. *The probability of the query $\hat{y}_i = y_i$ in the predictive checklist is given by*

$$P_{\mathcal{P}_\theta}(\hat{y}_i = 1) = 1 - P_{\mathcal{P}_\theta}(\hat{y}_i = 0) = \sum_{d=T}^{d'} \sum_{\sigma \in \Sigma^d} \prod_{j=1}^{d'} (\mathbf{p}_i[j])^{\sigma(j)} (1 - \mathbf{p}_i[j])^{1-\sigma(j)} \tag{2}$$

where Σ_d is the set of selection functions $\sigma : [d'] \to \{0,1\}$ such that $\sum_{j=1}^{d'} \sigma(j) = d$.

The detailed derivations are presented in Appendix A. We use the log-likelihood as the loss function, which leads our final loss: $\mathcal{L} = y_i \log(P_{\mathcal{P}_\theta}(\hat{y}_i = 1)) + (1 - y_i) \log(P_{\mathcal{P}_\theta}(\hat{y}_i = 0))$.

The parameters θ, include multiple elements: the parameters of the different soft concept extractors (θ_ψ), the number of concepts to be extracted for each data modality d'_k, the checklist threshold T. As the soft concept extractors are typically parameterized by neural networks, optimizing $\mathcal{L}$ with respect to θ_ψ can be achieved via gradient based methods. d'_k and T are constrained to be integers and are thus treated as hyper-parameters in our experiments.

4.5 Checklist Inference

ProbChecklist relies on soft concepts extraction for each data modality. Yet, at test time, a checklist operates on binary input data. We thus binarize the predicted soft concepts by setting $\mathbf{c}_i[j] =$

$\mathbb{I}[\mathbf{p}_i[j] > \tau]$. The thresholding parameter τ is an hyperparameter that can be tuned based on validation data. After training, we construct the final checklist by pruning the concepts that are never used in the training data (*i.e.* concepts j such that $\mathbf{c}_i[j] = 0, \forall i$, are pruned). This step offers users the flexibility to tune between sensitivity-specificity depending on the application. The optimal checklist can be obtained by varying τ to optimize the desired metric on the validation data.

4.6 Interpretability of the concept extractors

The checklist concepts are learnt using deep neural networks and are, therefore, not interpretable in general. To address this issue, we propose two mechanisms to improve the interpretability of the learnt concepts: *focused* concept learners and regularization terms that incorporate explainability in the structure of the concept learners. Focused models limit the range of features that can contribute to a concept. This can be done via manual specification of the models e.g. using different LSTMs for each time series (Johnson et al., 2022). Regularization terms such as TANGOS helps unveil each input signal's contribution to the learnt concepts for a given sample, making the concepts interpretable. It ensures that the concepts are obtained from distinct and sparse subsets of the input vector, avoiding overlap. Sparsity is achieved by taking the L1-norm of the concept gradient attributions with respect to the input vector. To promote decorrelation of signal learned in each concept, the loss is augmented by incorporating the inner product of the gradient attributions for all pairs of concepts. This scheme compels the models to learn unique concepts. More details about TANGOS and its mathematical formulation can be found in the Appendix F.1. We additionally introduce a regularization term which propels the learnt concept probabilities towards either 0 or 1. This term helps in identifying characteristic concepts for each patient: $\mathcal{L}_{prob-reg} = \sum_j \sum_i p_i[j]$.

4.7 Fairness Regularization

We encourage fairness of the learnt checklists by equalizing the error rate across subgroups of protected variables. This is achieved by penalizing significant differences in False Positive and False Negative Rates for sensitive subgroups (Pessach & Shmueli, 2022). For a binary classification problem, with protected attribute S, predicted labels $\hat{y} \in \{0, 1\}$, and actual label $y \in \{0, 1\}$, we define separations as follows (Corbett-Davies & Goel, 2018):

$$\Delta FPR = \|P(\hat{y}_i = 1|y = 0, S = s_i) - P(\hat{y}_i = 1|y = 0, S = s_j)\|_1 \ \ \forall s_i, s_j \in S \tag{3}$$

$$\Delta FNR = \|P(\hat{y}_i = 0|y = 1, S = s_i) - P(\hat{y}_i = 0|y = 1, S = s_j)\|_1 \ \ \forall s_i, s_j \in S \tag{4}$$

and combine these in a fairness regularizer $\mathcal{L}_{\text{Fair}} = \lambda(\Delta FPR + \Delta FNR)$.

5 Experiments

We investigate the performance of ProbChecklist along multiple axes. We first compare the classification performance against a range of interpretable machine learning baselines. Second, we investigate the importance of several key hyperparameters of our method. Lastly, we demonstrate how we can tune the interpretability of the learnt concepts and how we can enforce fairness constraints into ProbChecklist. Complete details about the datasets, baselines used in our experiments, and hyperparameter tuning are available in Appendix E, C.

Baselines. We compare our method against the following baselines.

Mixed Integer Programming (MIP)(Makhija et al., 2022). This approach allows to learn predictive checklists from continuous inputs. For images or time series, we typically apply MIP on top of an embedding obtained from a pre-trained deep learning model.

Integer Linear Program (ILP)(Zhang et al., 2021). ILP learns predictive checklists with Boolean inputs. We apply these to tabular data by categorizing the data using feature means as threshold.

CNN/LSTM/BERT + Logistic Regression (LR). This consists in using a CNN, LSTM or pre-trained BERT on the input data and applying a logistic regression on the combination of the last layer's embeddings of each modality.

CNN/LSTM/BERT + Multilayer perceptron (MLP). This is similar to the previous approach but where we apply an MLP on the combination of the last layer's embeddings of each modality.

Datasets. A crucial strength of our method resides in its ability to learn predictive from high dimensional input data. We briefly describe the MNIST synthetic dataset created here and defer the descriptions of other datasets (PhysioNet sepsis tabular dataset, MIMIC mortality dataset, Medical Abstracts TC Corpus) to the Appendix E.3

Synthetic MNIST checklist. Due to the absence of real-world datasets with ground-truth checklists, we first validate our idea on a synthetic setup created using MNIST image sequences as input and a checklist defined on digit labels. Each sample consists of a sequence of $\mathbf{K} = 4$ MNIST images (treating each image as a separate modality). We then assign a label to *each samples* according to the following ground-truth checklist. (i) Digit of $\mathbf{Image\,1} \in \{0, 2, 4, 6, 8\}$, (ii) $\mathbf{Image\,2} \in \{1, 3, 5, 7, 9\}$, (iii) $\mathbf{Image\,3} \in \{4, 5, 6\}$, (iv) $\mathbf{Image\,4} \in \{6, 7, 8, 9\}$. If at least 3 of the rules are satisfied, the label is 1, and 0 otherwise.

5.1 CHECKLIST PERFORMANCE

We evaluate the classification performance of the different models according to accuracy, precision, recall and specificity. For the checklist baselines, we also report the total number of concepts used (M) and the threshold for calling a positive sample (T). Results are presented in table 1. Additional results and details about hyperparameter tuning are provided in the Appendix E,C.

Dataset	Model	Accuracy	Precision	Recall	Specificity	$\mathbf{d'_k}$	T	M
MNIST Checklist	CNN + MLP	94.72 ± 4.32	0.895 ± 0.1	0.835 ± 0.13	0.976 ± 0.02	4	-	-
	CNN + LR	95.04 ± 0.31	0.914 ± 0.01	0.836 ± 0.016	**0.98 ± 0.003**		-	-
	pretrained CNN + MIP	79.56	0	0	1		8	13.5 ± 0.5
	ProbChecklist	**96.808 ± 0.24**	**0.917 ± 0.015**	**0.929 ± 0.01**	0.978 ± 0.004	4	8.4 ± 1.2	16
PhysioNet Tabular	Logistic Regression	62.555 ± 1.648	0.624 ± 0.0461	0.144 ± 0.0393	**0.9395 ± 0.0283**	1	-	-
	Unit Weighting	58.278 ± 3.580	0.521 ± 0.093	0.4386 ± 0.297	0.6861 ± 0.251		3.2 ± 1.16	9.6 ± 0.8
	ILP mean thresholds	62.992 ± 0.82	0.544 ± 0.087	0.1196 ± 0.096	0.9326 ± 0.0623		2.8 ± 0.748	4.4 ± 1.01
	MIP Checklist	**63.688 ± 2.437**	0.563 ± 0.050	**0.403 ± 0.082**	0.7918 ± 0.06		3.6 ± 0.8	8 ± 1.095
	ProbChecklist	62.579 ± 2.58	**0.61 ± 0.076**	0.345 ± 0.316	0.815 ± 0.185S	1	3.6 ± 1.2	10
MIMIC III	Unit Weighting	73.681 ± 0.972	0.469 ± 0.091	0.223 ± 0.206	0.889 ± 0.026	1	6.1 ± 0.830	8.9 ± 0.627
	ILP mean thresholds	75.492 ± 0.318	0.545 ± 0.028	0.142 ± 0.059	0.959 ± 0.019		3.6 ± 0.894	3.6 ± 0.894
	MIP Checklist	74.988 ± 0.025	0.232 ± 0.288	0.014 ± 0.017	**0.997 ± 0.004**		4.5 ± 2.082	4.5 ± 2.082
	LSTM + LR	66.585 ± 2.19	0.403 ± 0.02	**0.684 ± 0.039**	0.66 ± 0.034		-	-
	LSTM + MLP	76.128 ± 0.737	0.446 ± 0.223	0.23 ± 0.132	0.939 ± 0.036		-	-
	LSTM + MLP (all features)	**80.04 ± 0.598**	0.328 ± 0.266	0.129 ± 0.131	0.962 ± 0.043		-	-
	ProbChecklist	77.58 ± 0.481	**0.642 ± 0.075**	0.247 ± 0.032	0.953 ± 0.019	2	9.6	20
Medical Abstracts Corpus	BERT + ILP	72.991 ± 8.06	0.292 ± 0.29	0.197 ± 0.26	0.879 ± 0.17	6	1.2 ± 0.4	1.2 ± 0.4
	BERT + MIP	69.32 ± 8.1	0.583 ± 0.14	0.059 ± 0.08	0.991 ± 0.09		2.5 ± 0.6	4 ± 0.8
	BERT + LR	80.193 ± 0.88	**0.790 ± 0.051**	0.138 ± 0.065	**0.988 ± 0.007**		-	-
	BERT + MLP	81.782 ± 0.31	0.941 ± 0.04	0.07 ± 0.009	0.961 ± 0.01		-	-
	ProbChecklist	**83.213 ± 0.23**	0.616 ± 0.006	**0.623 ± 0.01**	0.891 ± 0.003	6	3	6

Table 1: Performance results for all the models and baselines on all the datasets. We report accuracy, precision, recall as well as conciseness of the learnt checklist. To facilitate visualization and comparison, we plot these results in Section I of the Appendix (Figure 10).

MNIST Checklist. We used a simple three-layered CNN model as the concept learner for each image. In Table 1, we report the results of the baselines and ProbChecklist for $\mathbf{d'_k} = \mathbf{4}$ $(\mathbf{M} = \mathbf{16})$ on the test samples. Our method outperforms all the baselines, in terms of accuracy and recall, indicating that it identifies the minority class better than these standard approaches. The MIP failed to find solutions for some folds of the dataset and didn't generalise well on the test samples.

Sepsis Prediction from Tabular Data. This setup is ideal for comparison with existing checklist method as they only operate on tabular dataset. In Figure 4, we visualize learnt by ProbChecklist in one of the experiments. We observe that ProbChecklist exhibits similar performance to checklist baselines. We want to emphasize that ProbChecklist provides a significantly broader applicability to multimodal datasets while maintaining comparable performance on tabular datasets, thus making it valuable.

Neoplasm Detection from Clinical Abstracts. We use a pretrained BERT model (Alsentzer et al., 2019) with frozen weights as our concept learner. This was a BioBERT model pretrained on clinical notes of MIMIC-III dataset. Our checklist has a much better recall and accuracy than previous methods. Both checklist learning and deep learning methods give poor performance on the minority class.

Mortality Prediction using Time Series Data. To learn representations from clinical timeseries, we initialize K two-layered LSTMs. We highlight our key results in Table 1. For ProbChecklist, we report the checklist which attains the highest accuracy on validation data. We surpass existing methods in terms of accuracy and precision with a significant margin. We find that a checklist with better recall can be constructed by optimizing over F1-Score instead of accuracy.

Sensitivity analysis: We investigate the evolution of performance of ProbChecklist with increasing number of learnt concepts $\mathbf{d'_k}$. On Figure 3a, we show the accuracy, precision, recall, and specificity

in function of the number of concepts per image on the MNIST dataset. We observe a significant improvement in performance when $\mathbf{d'_k}$ increases from $\mathbf{1}$ to $\mathbf{2}$, which suggests that having learning one concept per image is inadequate to capture all the signal in the sample. It is also interesting to note that the performance reaches a saturation point after $\mathbf{d'_k} = 3$. This suggests held-out loss can be used to tune the value of $\mathbf{d'_k}$ to find the optimal number of concepts for a given data modality.

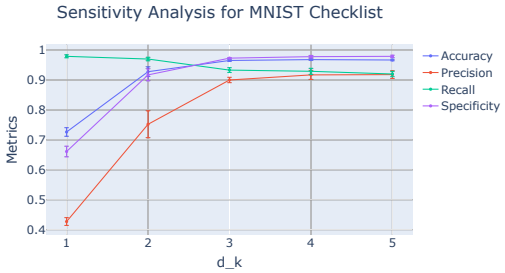

(a) Performance of ProbChecklist with varying $\mathbf{d'_k}$ on MNIST Checklist Dataset

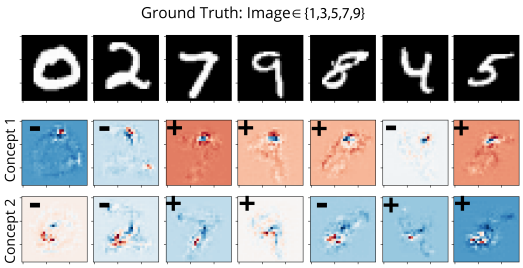

(b) We plot images and corresponding gradient attributions heat maps for seven inputs samples of the Image 2 modality of the MNIST dataset. We used a checklist with two learnable concepts per image. The intensity of red denotes the positive contribution of each pixel, whereas blue indicates the negative. If a concept predicted as true for an image, then we represent that with plus (+) sign, and with a negative sign (-) otherwise.

Figure 3

5.2 Concepts Interpretation

We investigate the concepts learnt from image and timeseries datasets with an interpretability regularization as in Section 4.6. To gain insight into what patterns of signals refer to each individual concept, we examine the gradient of each concept with respect to each dimension of the input signal. Intuitively, the interpretability regularization enforces the concepts to focus on a sparse set of features of the input data.

MNIST Images: We analyze the gradient of our checklist on individual pixels of the input images. We use a checklist with two concepts per image. On Figure 3b, we show example images of the *Image 2* of the MNIST dataset along with the gradient heat map for each learnt concept of the checklist. The ground truth concept for this image is $\mathbf{Image\,2} \in \{1, 3, 5, 7, 9\}$. First, we see that the $7, 9$, and 5 digits are indeed the only ones for which the predicted concepts of our checklist are positive. Second, we infer from the gradient heat maps that concepts 1 and 2 focus on the image's upper half and centre region, respectively. Concept 1 is true for digits 5, 8, 9 and 7, indicating that it corresponds to a horizontal line or slight curvature in the upper half. Since Digits 0 and 2 have deeper curvature than the other images, and there is no activity in that region in the case of 4, concept 1 is false for them. concept 2 is true for images with a vertical line, including digits 9, 4, 5 and 7. Therefore, concept 2 is false for the remaining digits (0, 2, 8). The checklist outcome matches the ground truth when both concepts are true for a given image. Complementary analyses on MNIST and MIMIC III are provided in Appendix F.2 and F.3. This analysis ensures interpretability at the individual sample level. As illustrated in the previous example, recognizing and comprehending these concepts at the dataset level relies on visual inspection.

Medical Abstracts: Compared to images and time series, interpreting concepts learned from textual data is easier because its building blocks are tokens which are already human understandable. For the Neoplasm detection task, we adopt an alternative method by conducting a token frequency analysis across the entire dataset. This approach has yielded a more lucid checklist shown in Figure 1. We identified key tokens associated with positive and negative concepts (positive and negative tokens). Each concept is defined by the presence of positive words and the absence of negative words.

5.3 Fairness

We evaluate the fairness of ProbChecklist on the MIMIC-III Mortality Prediction task and show that we can reduce the performance disparities between sensitive attributes by incorporating fairness regularization (FR) terms, as introduced in Section 4.7. We set the sensitive features as gender

$\in \{Male, Female\}$ and ethnicity $\in \{Black, White, Others\}$. Our results are displayed on Tables 2 and 11. These disparities in performance across different sub-populations are significantly reduced after fairness regularization is used. To see the effectiveness of the regularizer, we report the percentage decrease in ΔFNR and ΔFPR observed with respect to the unregularized checklist predictions for all pairs of sensitive subgroups. Similar fairness constraints (FC) can also be added to the ILP mean-thresholds baseline (Jin et al., 2022). We include a separate constraint for each pair that restricts |ΔFNR| and |ΔFPR| to be less than ϵ = 0.05.

It is important to note that our approach minimizes the summation of ΔFNR and ΔFPR across all pairs of subgroups, but in the ILP we can specify a strict upper bound for each pair. Due to this, we might observe an increase in the gap for certain pairs in case of ProbChecklist, but adjusting the relative weights of these terms in the loss equation helps in achieving optimal performance. Although ProbChecklist had higher initial FNR/FPR values, the regularizer effectively reduces them to be comparable to those of ILP, particularly for the ethnicity pairs.

Sepsis if 3+ items are true

- ☐ **Bilirubin direct sd** ≥ 1.31
- ☐ **FiO2 sd** ≥ 0.029
- ☐ **FiO2 mean** ≥ 0.035
- ☐ **EtCO2 sd** ≥ 0
- ☐ **FiO2 last** ≥ 0.037
- ☐ **Alkalinephos sd** ≥ 0
- ☐ **AST sd** ≥ 0
- ☐ **pH sd** ≥ 0.221
- ☐ **TroponinI sd** ≥ 0
- ☐ **Bilirubin direct last** ≥ 7.352

Figure 4: Learnt checklist for PhysioNet Sepsis Prediction Task (Tabular). We report the performance result as accuracy (65.69%), precision (0.527), recall (0.755), and specificity (0.6).

6 DISCUSSION

Performance of ProbChecklist. Through these experiments, we aim to showcase that ProbChecklist surpasses existing checklist methods and achieves comparable performance to MLP (non-interpretable) methods. The switch to learnable concepts explains the improvement in accuracy over checklist methods. These concepts capture more signal than fixed summary/concept extractors used in prior works to create binarized tabular data. It's important to note that a checklist, due to its binary weights, has a strictly lower capacity and is less expressive than deep learning but possesses a more practical and interpretable structure. Despite this, it exhibits similar performance to an MLP.

Interpretability of checklist structure and learnt concepts. Although ProbChecklist employs a probabilistic objective for training the concept learners, the end classifier used for inference is, in fact, a discrete checklist. While this makes the classifier highly interpretable, it also shifts the focus of interpretability to the learnt concepts. We fully realize this trade-off and investigate existing techniques to maintain feature-space interpretability. For time series and images, we employ regularization terms (4.6) to enforce sparsity, avoid redundancy, and learn strongly discriminative features with high probability. We also use focused concept learners to avoid learning concepts that are functions of multiple modalities. Identifying patterns from the binarized concepts is primarily based on visual inspection and expert knowledge. We noticed it is easier to source and comprehend the key tokens contributing to each concept for text data. Lastly, we want to highlight that ProbChecklist is a flexible framework, and other interpretable models can be easily integrated as concept learners.

	Method	Female-Male		White-Black		Black-Others		White-Others	
		ΔFNR	ΔFPR	ΔFNR	ΔFPR	ΔFNR	ΔFPR	ΔFNR	ΔFPR
ILP mean thresholds	w/o FC	0.038	0.011	0.029	0.026	0.152	0.018	0.182	0.045
	FC	0.011	0.001	0.031	0.008	0.049	0.016	0.017	0.0007
	% $\downarrow$	71.053	90.909	-6.897	69.231	67.763	11.111	90.659	98.444
ProbChecklist	w/o FR	0.127	0.311	0.04	0.22	0.02	0.273	0.02	0.053
	FR	0.103	0.089	0.028	0.016	0.021	0.008	0.006	0.008
	% $\downarrow$	18.898	71.383	30.000	92.727	-5.000	97.033	70.000	85.660

Table 2: Improvement in fairness metrics across gender and ethnicity on MIMIC III for the mortality prediction task after adding fairness regularization. We report ΔFNR and ΔFPR for all pairs of subgroups of sensitive features and the percentage decrease (% $\downarrow$) wrt unregularized checklist.

Limitations. We have taken the first step towards learning checklists from complex modalities, whereas the existing methods are restricted to tabular data. Even though we have a mechanism to learn interpretable checklist classifiers using logical reasoning, more work is needed on the interpretability of the learnt concepts. Another drawback is the exponential memory complexity of the training. A fruitful future direction would be to study approximations to explore a smaller set of combinations of concepts. Detailed complexity analysis can be found in Appendix B.

Societal Impact. As discussed initially in the paper, manually designed checklists are extensively used in hospitals for decision-making under complex situations and help automate certain aspects of the treatment. With more research on the interpretability of concepts, ProbChecklist can replace the existing manual procedure and reduce the burden on the healthcare system.

REFERENCES

Muhammad Aurangzeb Ahmad, Carly Eckert, and Ankur Teredesai. Interpretable machine learning in healthcare. In *Proceedings of the 2018 ACM international conference on bioinformatics, computational biology, and health informatics*, pp. 559–560, 2018.

Emily Alsentzer, John Murphy, William Boag, Wei-Hung Weng, Di Jin, Tristan Naumann, and Matthew McDermott. Publicly available clinical BERT embeddings. In *Proceedings of the 2nd Clinical Natural Language Processing Workshop*, pp. 72–78, Minneapolis, Minnesota, USA, June 2019. Association for Computational Linguistics. doi: 10.18653/v1/W19-1909. URL https://www.aclweb.org/anthology/W19-1909.

Alejandro Barredo Arrieta, Natalia Díaz-Rodríguez, Javier Del Ser, Adrien Bennetot, Siham Tabik, Alberto Barbado, Salvador García, Sergio Gil-López, Daniel Molina, Richard Benjamins, et al. Explainable artificial intelligence (xai): Concepts, taxonomies, opportunities and challenges toward responsible ai. *Information fusion*, 58:82–115, 2020.

Adrien Bennetot, Jean-Luc Laurent, Raja Chatila, and Natalia Díaz-Rodríguez. Towards explainable neural-symbolic visual reasoning. *arXiv preprint arXiv:1909.09065*, 2019.

Sam Corbett-Davies and Sharad Goel. The measure and mismeasure of fairness: A critical review of fair machine learning, 2018.

Thomas Davenport and Ravi Kalakota. The potential for artificial intelligence in healthcare. *Future healthcare journal*, 6(2):94, 2019.

Edward De Brouwer, Javier Gonzalez, and Stephanie Hyland. Predicting the impact of treatments over time with uncertainty aware neural differential equations. In *International Conference on Artificial Intelligence and Statistics*, pp. 4705–4722. PMLR, 2022.

Luc De Raedt and Angelika Kimmig. Probabilistic (logic) programming concepts. *Machine Learning*, 100(1):5–47, 2015.

Mengnan Du, Ninghao Liu, and Xia Hu. Techniques for interpretable machine learning. *Communications of the ACM*, 63(1):68–77, 2019.

Andre Esteva, Alexandre Robicquet, Bharath Ramsundar, Volodymyr Kuleshov, Mark DePristo, Katherine Chou, Claire Cui, Greg Corrado, Sebastian Thrun, and Jeff Dean. A guide to deep learning in healthcare. *Nature medicine*, 25(1):24–29, 2019.

Ashraf Fawzy, Tianshi David Wu, Kunbo Wang, Matthew L. Robinson, Jad Farha, Amanda Bradke, Sherita H. Golden, Yanxun Xu, and Brian T. Garibaldi. Racial and Ethnic Discrepancy in Pulse Oximetry and Delayed Identification of Treatment Eligibility Among Patients With COVID-19. *JAMA Internal Medicine*, 182(7):730–738, 07 2022. ISSN 2168-6106. doi: 10.1001/jamainternmed.2022.1906. URL https://doi.org/10.1001/jamainternmed.2022.1906.

Joseph Futoma, Morgan Simons, Trishan Panch, Finale Doshi-Velez, and Leo Anthony Celi. The myth of generalisability in clinical research and machine learning in health care. *The Lancet Digital Health*, 2(9):e489–e492, 2020.

Marzyeh Ghassemi, Tristan Naumann, Peter Schulam, Andrew L Beam, Irene Y Chen, and Rajesh Ranganath. A review of challenges and opportunities in machine learning for health. *AMIA Summits on Translational Science Proceedings*, 2020:191, 2020.

Brigette Hales, Marius Terblanche, Robert Fowler, and William Sibbald. Development of medical checklists for improved quality of patient care. *International Journal for Quality in Health Care*, 20(1):22–30, 12 2007. ISSN 1353-4505. doi: 10.1093/intqhc/mzm062. URL https://doi.org/10.1093/intqhc/mzm062.

Brigette Hales, Marius Terblanche, Robert Fowler, and William Sibbald. Development of medical checklists for improved quality of patient care. *International Journal for Quality in Health Care*, 20(1):22–30, 2008.

Alex B Haynes, Thomas G Weiser, William R Berry, Stuart R Lipsitz, Abdel-Hadi S Breizat, E Patchen Dellinger, Teodoro Herbosa, Sudhir Joseph, Pascience L Kibatala, Marie Carmela M Lapitan, et al. A surgical safety checklist to reduce morbidity and mortality in a global population. *New England journal of medicine*, 360(5):491–499, 2009.

Alan Jeffares, Tennison Liu, Jonathan Crabbé, Fergus Imrie, and Mihaela van der Schaar. TANGOS: Regularizing tabular neural networks through gradient orthogonalization and specialization. In *The Eleventh International Conference on Learning Representations*, 2023. URL https://openreview.net/forum?id=n6H86gW8u0d.

Qixuan Jin, Haoran Zhang, Thomas Hartvigsen, and Marzyeh Ghassemi. Fair multimodal checklists for interpretable clinical time series prediction. In *NeurIPS 2022 Workshop on Learning from Time Series for Health*, 2022. URL https://openreview.net/forum?id=y4mt_fTy6MY.

Alistair E.W. Johnson, Tom J. Pollard, Lu Shen, Li-wei H. Lehman, Mengling Feng, Mohammad Ghassemi, Benjamin Moody, Peter Szolovits, Leo Anthony Celi, and Roger G. Mark. Mimic-iii, a freely accessible critical care database. *Scientific Data*, 3(1), 2016. doi: 10.1038/sdata.2016.35.

Nari Johnson, Sonali Parbhoo, Andrew Ross, and Finale Doshi velez. Learning predictive and interpretable timeseries summaries from icu data. *AMIA ... Annual Symposium proceedings. AMIA Symposium*, 2021:581–590, 02 2022.

Pang Wei Koh, Thao Nguyen, Yew Siang Tang, Stephen Mussmann, Emma Pierson, Been Kim, and Percy Liang. Concept bottleneck models. 2020.

Daphne Koller, Nir Friedman, Sašo Džeroski, Charles Sutton, Andrew McCallum, Avi Pfeffer, Pieter Abbeel, Ming-Fai Wong, Chris Meek, Jennifer Neville, et al. *Introduction to statistical relational learning*. MIT press, 2007.

Himabindu Lakkaraju, Stephen H. Bach, and Jure Leskovec. Interpretable decision sets: A joint framework for description and prediction. In *Proceedings of the 22nd ACM SIGKDD International Conference on Knowledge Discovery and Data Mining*, KDD '16, pp. 1675–1684, New York, NY, USA, 2016. Association for Computing Machinery. ISBN 9781450342322. doi: 10.1145/2939672.2939874. URL https://doi.org/10.1145/2939672.2939874.

Yukti Makhija, Edward De Brouwer, and Rahul G Krishnan. Learning predictive checklists from continuous medical data. *arXiv preprint arXiv:2211.07076*, 2022.

Robin Manhaeve, Sebastijan Dumancic, Angelika Kimmig, Thomas Demeester, and Luc De Raedt. Deepproblog: Neural probabilistic logic programming. *Advances in Neural Information Processing Systems*, 31, 2018.

W James Murdoch, Chandan Singh, Karl Kumbier, Reza Abbasi-Asl, and Bin Yu. Definitions, methods, and applications in interpretable machine learning. *Proceedings of the National Academy of Sciences*, 116(44):22071–22080, 2019.

Martijn Oldenhof, Ádám Arany, Yves Moreau, and Edward De Brouwer. Weakly supervised knowledge transfer with probabilistic logical reasoning for o-object detection. *International Conference on Learning Representations (ICLR)*, 2023.

Adam Paszke, Sam Gross, Francisco Massa, Adam Lerer, James Bradbury, Gregory Chanan, Trevor Killeen, Zeming Lin, Natalia Gimelshein, Luca Antiga, Alban Desmaison, Andreas Kopf, Edward Yang, Zachary DeVito, Martin Raison, Alykhan Tejani, Sasank Chilamkurthy, Benoit Steiner, Lu Fang, Junjie Bai, and Soumith Chintala. Pytorch: An imperative style, high-performance deep learning library. In *Advances in Neural Information Processing Systems 32*, pp. 8024–8035. Curran Associates, Inc., 2019. URL http://papers.neurips.cc/paper/9015-pytorch-an-imperative-style-high-performance-deep-learning-library.pdf.

Dana Pessach and Erez Shmueli. A review on fairness in machine learning. *ACM Comput. Surv.*, 55 (3), feb 2022. ISSN 0360-0300. doi: 10.1145/3494672. URL https://doi.org/10.1145/3494672.

Luc De Raedt, Kristian Kersting, Sriraam Natarajan, and David Poole. Statistical relational artificial intelligence: Logic, probability, and computation. *Synthesis lectures on artificial intelligence and machine learning*, 10(2):1–189, 2016.

Matthew A Reyna, Chris Josef, Salman Seyedi, Russell Jeter, Supreeth P Shashikumar, M Brandon Westover, Ashish Sharma, Shamim Nemati, and Gari D Clifford. Early prediction of sepsis from clinical data: the physionet/computing in cardiology challenge 2019. In *2019 Computing in Cardiology (CinC)*, pp. Page–1. IEEE, 2019.

Tim Rocktäschel and Sebastian Riedel. End-to-end differentiable proving. *Advances in neural information processing systems*, 30, 2017.

Adam Santoro, David Raposo, David G Barrett, Mateusz Malinowski, Razvan Pascanu, Peter Battaglia, and Timothy Lillicrap. A simple neural network module for relational reasoning. *Advances in neural information processing systems*, 30, 2017.

Tim Schopf, Daniel Braun, and Florian Matthes. Evaluating unsupervised text classification: Zero-shot and similarity-based approaches. In *Proceedings of the 2022 6th International Conference on Natural Language Processing and Information Retrieval*, NLPIR '22, pp. 6–15, New York, NY, USA, 2023. Association for Computing Machinery. ISBN 9781450397629. doi: 10.1145/3582768.3582795. URL https://doi.org/10.1145/3582768.3582795.

Maayan Shvo, Andrew C. Li, Rodrigo Toro Icarte, and Sheila A. McIlraith. Interpretable sequence classification via discrete optimization. In *Proceedings of the 35th AAAI Conference on Artificial Intelligence (AAAI)*, 2021. URL https://ojs.aaai.org/index.php/AAAI/article/view/17161.

Shirly Wang, Matthew BA McDermott, Geeticka Chauhan, Marzyeh Ghassemi, Michael C Hughes, and Tristan Naumann. Mimic-extract: A data extraction, preprocessing, and representation pipeline for mimic-iii. In *Proceedings of the ACM Conference on Health, Inference, and Learning*, pp. 222–235, 2020.

Tong Wang, Cynthia Rudin, Finale Doshi-Velez, Yimin Liu, Erica Klampfl, and Perry MacNeille. A bayesian framework for learning rule sets for interpretable classification. *Journal of Machine Learning Research*, 18(70):1–37, 2017. URL http://jmlr.org/papers/v18/16-003.html.

Haoran Zhang, Quaid Morris, Berk Ustun, and Marzyeh Ghassemi. Learning optimal predictive checklists. *Advances in Neural Information Processing Systems*, 34:1215–1229, 2021.

Quanshi Zhang, Ying Nian Wu, and Song-Chun Zhu. Interpretable convolutional neural networks. In *Proceedings of the IEEE Conference on Computer Vision and Pattern Recognition (CVPR)*, June 2018.

Appendix

A Derivations for the loss function

Given the individual probabilities of each concept j being positive, $\mathbf{p}_i[j]$, the probability that the checklist outputs exactly d positive concepts for sample i is given by the binomial distribution:

$$P_{\mathcal{P}_\theta}(\#\text{ true concepts} = d) = \sum_{\sigma \in \Sigma^d} \prod_{j=1}^{d'} (\mathbf{p}_i[j])^{\sigma(j)} (1 - \mathbf{p}_i[j])^{1-\sigma(j)},$$

where Σ_d is the set of selection functions $\sigma : [d'] \to \{0, 1\}$ such that $\sum_{j=1}^{d'} \sigma(j) = d$. The probability that the checklist gives a positive prediction is the probability that the number of positive concepts is larger than T, we thus have

$$P_{\mathcal{P}_\theta}(\hat{y}_i = 1) = \sum_{d=T}^{d'} \sum_{\sigma \in \Sigma^d} \prod_{j=1}^{d'} (\mathbf{p}_i[j])^{\sigma(j)} (1 - \mathbf{p}_i[j])^{1-\sigma(j)}.$$

B COMPLEXITY ANALYSIS

Let d be the number of positive concepts for sample i. Probabilistic Checklist Objective is defined as $P(d \geq T)$, i.e. the sample is classified as positive if T or more concepts (out of M) are true. We discuss the space and time complexity for training and inference separately.

Step-wise Breakdown for Training.

- **Learning concepts probabilities using a concept learner.** The computational complexity is contingent upon the specific neural network employed. In our analysis, we utilize LSTMs, CNNs, and pre-trained BERT models with fixed weights, ensuring that computations can be performed in polynomial time.
- **Loss computation.** We need to compute the probabilistic query $\mathbf{P}(\mathbf{d} \geq \mathbf{T})$. This involves iterating over all possible 2^M combinations of true concepts $\forall\ d \geq T$. The probability of each combination is obtained by taking product of concept probabilities.
  Worst case time complexity: $\mathbf{O}(\mathbf{M2^M}) \implies$ **exponential**.

We implement the time-efficient $\mathbf{O}(\mathbf{1})$ version of this method by caching the combination tensor in memory. In this situation, the memory cost becomes $\mathbf{O}(\mathbf{M2^M})$. The dimensions of tensor that stores all the combinations is $[2^M, M]$. This is an acceptable trade-off as it enables us to run experiments in reasonable time.

Inference. Inference involves a single pass through the concept learner. Since loss does not need to be computed, the inference time is the same for both memory- and time-efficient implementations of ProbChecklist and has the same complexity as the forward propagation of the concept learner.

Training Details.

We trained the time-efficient implementation with memory complexity $O(M * 2^M)$ on one NVIDIA A40 GPU with 48GB memory which can fit up to $M = 30$. Exponential complexity is primary reason for performing feature selection and limiting the modalities to 10 and learning up to 3 features per modality.

Training Time (seconds)	Number of concepts	MIP Checklist	ProbChecklist
PhysioNet Tabular ($d'_k = 1$)	10	667 ± 80.087	995.0 ± 35.014
MNIST (d'_k = 4)	16	3600	2773 ± 22.91

Table 3: ProbChecklist exhibits exponential complexity. To gauge the impact of this limitation, we provide training times (in seconds) for both MIP Checklist and ProbChecklist. It's crucial to highlight that while MIP Checklist performs effectively with tabular data, successfully uncovering the optimal solution, its performance is poor when applied to MNIST synthetic setup. Even when we set the runtime for Gurobi solver as 1 hour, it struggles to achieve optimal solutions for many cases. On the other hand, ProbChecklist stands out as more reliable, capable of performing end-to-end training and successfully learning the optimal solution.

A fruitful future direction would be to study approximations to explore a smaller set of combinations.

C HYPERPARAMETER TUNING

ProbChecklist framework allows experts to design user-centric checklists. Hyperparameters d'_k, $Tand\ M$ represent the structure/compactness of the checklist but alone aren't sufficient to garner information about the checklist's performance. Different d'_k are tried for each modality in an increasing fashion to find the one that performs best. Sensitivity analysis to study the relation between

d'_k and performance (Figure 3a) suggests that the performance saturates after a certain point. This point can be determined experimentally for different modalities. M, total concepts in the checklist, is obtained by pruning concepts that are true for insignificant samples. Our experiments showed that pruning was not required since all the concepts were true for a significant fraction of samples. This indicates the superior quality of the concepts.

We try different values of T in the range [M/4, M/2] (total items M) to find the most performant model. However, this hyperparameter tuning doesn;t contribute to the computational cost. For d'_k, we only only 2-3 values, and use the same value for all the features. Domain experts will be more equipped to choose these values based on their knowledge of the features. For example, if we are recording a time series feature known to stay stable (not fluctuate much), then low d'_k is sufficient. The value of d'_k also depends on the number of observations (most blood tests aren't performed hourly, but heart rate and oxygen saturation are monitored continuously).

D CONCISENESS OF CHECKLISTS OVER DECISION TREES

Decision trees represent another highly interpretable classification method. Compared to checklists, they strike a different balance between expressivity and conciseness. While trees grow exponentially with the number of rules, checklists only grow linearly. Yet, the increased complexity of trees makes them also more expressive. Each decision in a tree only applies to its specific lineage. In contrast, each rule in a checklist applies globally. Despite their lower expressivity, the conciseness of checklists can make them more practical and interpretable than decision trees.

E EXPERIMENT DETAILS

In this section we provide additional details about the experiments.

E.1 BASELINES

We compare the performance of our method against standard classifiers, including logistic regression (LR) and a classical multilayer perceptron (MLP). For a fair comparison, the process to obtain the M-dimensional concept probabilities is identical for all methods.

For the clinical datasets, we also use architectures tailored for learning checklists, namely Unit weighting, SETS checklist, Integer Linear Program (Zhang et al., 2021) with mean thresholds, and MIP from Makhija et al. (2022). These checklist-specific architectures lack the ability to process complex data modalities such as time series data, so we use features mean values for training them.

Unit weighting distils a pre-trained logistic regression into a checklist, as also used in Zhang et al. (2021). First, we binarise the data by using the mean feature values as thresholds. By training a simple logistic regression on the continuous data, we can determine the features with negative weights and replace them with their complements. A hyperparameter β to discard features with weights in the range $[-\beta, \beta]$. Subsequently, we train logistic regression models on the binarized data by varying $T \in [0, M]$ (the checklist threshold) to identify the optimal value of T.

SETS checklist (Makhija et al., 2022) is an improvement over Unit Weighting, where mean values are directly utilized for binarization. This method aims to learn feature thresholds (μ) while training a logistic regression in a temperature parameter (τ) followed by unit weighting to generate the checklist.

$$\sigma(\frac{X-\mu}{\tau}) \quad \text{where, } \sigma \text{ sigmoid function.} \tag{5}$$

For **Integer Linear Program with Mean Thresholds**, we re-implement the ILP from Zhang et al. (2021) on the mean binarized data and solve the optimization problem using Gurobi. Comparing our method to this baseline provides the most relevant benchmark for evaluation.

Mixed Integer Program (Makhija et al., 2022) is a modification of the ILP described above and contains additional constraints to learn thresholds instead of using fixed ones. Again, we re-implement the optimization problem and solve it on Gurobi.

BERT/LSTM/CNN + LR employs the concept learners used in ProbChecklist followed by a logistic regression layer on the combination of last layer's embeddings for each modality. Finally, cross-entropy loss is calculated on the predicted class, i.e. $\mathbb{P}(\hat{\mathbf{y}} = \mathbf{1})$.

E.2 Reasons for creating MNIST synthetic Dataset

Since there aren't any real-world datasets with a ground truth checklist, we first validate our idea on a synthetic setup where the checklist is known. The key points we examine were the performance of our probabilistic checklist objective compared to standard MLP and LR architectures, the comprehensibility of the concepts learnt, and how well our approach recovers the defined rules.

The ideal dataset needed to substantiate our approach comprises different features (or modalities) and a defined rule/condition for each modality to assign the samples a ground truth label. Similar to the structure of a checklist, the sample label depends on how many rules.

These points were taken into account while designing the MNIST Synthetic Checklist.

E.3 Datasets

MNIST Checklist Dataset
We generate a synthetic dataset from MNIST and define a rule set based on which the instances are classified as 0 or 1. We divide all the images in the MNIST dataset into sequences of $\mathbf{K}$ images, and each sequence forms one sample. In the experiments, we set $\mathbf{K} = \mathbf{4}$, which creates a dataset consisting of 10500 samples for training, 4500 for validation, and 2500 for testing. We start by learning $\mathbf{M}$ concepts from images directly using $\mathbf{K}$ concepts learners, which will later be used for recovering the set checklist. Concept learners would ensure that additional information beyond the labels is also captured.

We construct a ground truth checklist using the image labels to simulate a binary classification setup. A sample is assigned $\mathbf{y} = +\mathbf{1}$ if $\mathbf{T}$ out of $\mathbf{K}$ items are true. The final checklist used for experimentation is:

- **Ground Truth Checklist ($\mathbf{T} = 3$, $\mathbf{K} = 4$)**
  - ☐ $\mathbf{Image\,1} \in \{0, 2, 4, 6, 8\}$
  - ☐ $\mathbf{Image\,2} \in \{1, 3, 5, 7, 9\}$
  - ☐ $\mathbf{Image\,3} \in \{4, 5, 6\}$
  - ☐ $\mathbf{Image\,4} \in \{6, 7, 8, 9\}$

The final dataset contains 20.44% positive samples.

PhysioNet Sepsis Tabular Dataset
We use the PhysioNet 2019 Early Sepsis Prediction time series dataset (Reyna et al., 2019), which was collected from the ICUs of three hospitals. Hourly data of vital signs and laboratory tests are available for the thirty-four non-static features in the dataset. Additionally, four static parameters, gender, duration, age, and anomaly start point, are included. We treat the occurrence of sepsis in patients as the binary outcome variable.

The original dataset contains 32,268 patients, with only 8% sepsis patients. We create five subsets with 2200 patients, of which nearly 37% are positive. For this task, we use basic summary extraction functions such as the mean, standard deviation, and last entry of the clinical time series of each patient to tabulate the dataset. We subsequently perform feature selection and only keep the top ten informative features ($\mathbf{K} = \mathbf{10}$) based on logistic regression weights.

PhysioNet Sepsis Time Series Data
We use the PhysioNet 2019 Early Sepsis Prediction (Reyna et al., 2019) for this task also. The preprocessing steps and formation of subsets are the same as described above. Instead of computing summary statistics from the clinical time series, we train different concept learners to capture the dynamics of the time series. This allows us to encapsulate additional information, such as sudden rise or fall in feature values as concepts.

The processed dataset contains 2272 training, 256 validation, 256 testing samples, and 56 time steps for each patient. We fix $\mathbf{K} = \mathbf{10}$, i.e. use the top ten out of thirty-four features based on logistic

regression weights. The selected features are {temperature, TroponinI, FiO2, WBC, HCO3, SaO2, Calcium, HR, Fibrinogen, AST}.

MIMIC-III Mortality Time Series Data
We use the clinical time series data from the MIMIC III Clinical Database (Johnson et al., 2016) to perform mortality prediction on the data collected at the intensive care facilities in Boston. We directly use the famous MIMIC-Extract (Wang et al., 2020) preprocessing and extraction pipeline to transform the raw Electronic Medical Records consisting of vital signs and laboratory records of more than 50,000 into a usable time series format. The processed dataset had a severe class imbalance with respect to the mortality prediction task. We randomly sample from the negative class to increase the percentage to 25% positive patients. Subsequently, we divide the samples into training, validation, and test subsets comprising 6912, 768, and 2048 patients. Like the PhysioNet experiments, we retain the top ten time-series features ($\mathbf{K = 10}$). These features are {heart rate, mean blood pressure, diastolic blood pressure, oxygen saturation, respiratory rate, glucose, blood urea nitrogen, white blood cell count, temperature, creatinine}. To evaluate the proposed fairness regularizer, we introduce the one-hot encodings of two categorical features, gender and ethnicity.

Medical Abstracts TC Corpus. We work with the clinical notes dataset designed for multi-class disease classification (Schopf et al., 2023). However, we only focus on neoplasm detection. This subset contains 14438 total samples consisting of 11550 training samples and 2888 testing samples. Out of these, 2530 were positive in training set and 633 were positive in the testing set. To reduce class imbalance of 21.9%, the negative set was subsampled to result in an ratio of positive samples to negative samples of 35%. We use medical abstracts which describe the conditions of patients. Each note is 5-6 sentences long on average. We consider the whole text as one modality ($\mathbf{K = 1}$).

E.4 Sepsis Prediction using Static Tabular Data

Data. We use the PhysioNet 2019 Early Sepsis Prediction time series dataset (Reyna et al., 2019). We transformed this dataset into tabular data by using basic summary extraction functions such as the mean, standard deviation, and last entry of the clinical time series of each patient. We subsequently perform feature selection and only keep the top ten informative features ($\mathbf{K = 10}$) based on logistic regression weights.

Architecture. Since each feature is simply a single-valued function ($\mathbf{x_i} \in \mathbb{R}$), the concept learners are single linear layers followed by a sigmoid activation function. The remaining steps are the same as the previous task, i.e. these concept probabilities are then passed to the probabilistic logic module for $\mathbb{P}(\mathbf{d} > \mathbf{T})$ computation and loss backpropagation.

Baselines. We use standard baselines like MLP and LR, along with checklist-specific architectures, namely Unit weighting, SETS checklist, Integer Linear Program (Zhang et al., 2021) with mean thresholds, MIP from Makhija et al. (2022). Unit weighting distils a pre-trained logistic regression into a checklist, as also used in Zhang et al. (2021). SETS checklist (Makhija et al., 2022) consists of a modified logistic regression incorporating a temperature parameter to learn feature thresholds for binarization, this is followed by unit weighting.

Results. We present the results of ProbChecklist and baselines in Table 4. Our performance is slightly lower than the MIP baseline. The highest accuracy is achieved by an MLP, but that comes at the cost of lower interpretability.

Model	Accuracy	Precision	Recall	Specificity	M	T
Dummy Classifier	37.226	0.372	1	0.628	-	-
MLP Classifier	**64.962 ± 2.586**	0.5726 ± 0.046	0.483 ± 0.074	0.76043 ± 0.0562	-	-
Logistic Regression	62.555 ± 1.648	0.624 ± 0.0461	0.144 ± 0.0393	**0.9395 ± 0.0283**	-	-
Unit Weighting	58.278 ± 3.580	0.521 ± 0.093	0.4386 ± 0.297	0.6861 ± 0.251	9.6 ± 0.8	3.2 ± 1.16
SETS Checklist	56.475 ± 7.876	0.517 ± 0.106	**0.6639 ± 0.304**	0.494 ± 0.3195	10 ± 0	6 ± 0.632
ILP mean thresholds	62.992 ± 0.82	0.544 ± 0.087	0.1196 ± 0.096	0.9326 ± 0.0623	4.4 ± 1.01	2.8 ± 0.748
MIP	63.688 ± 2.437	0.563 ± 0.050	0.403 ± 0.082	0.7918 ± 0.06	8 ± 1.095	3.6 ± 0.8
Concepts + LR	61.168 ± 1.45	0.565 ± 0.059	0.324± 0.15	0.805 ± 0.1	-	-
ProbChecklist	62.579 ± 2.58	**0.61 ± 0.076**	0.345 ± 0.316	0.815 ± 0.185S	10	3.6 ± 1.2

Table 4: Performance results for Sepsis Prediction task using Tabular Data.

E.5 SEPSIS PREDICTION USING TIME SERIES DATA

Instead of computing summary statistics from the clinical time series, we train different concept learners to capture the dynamics of the time series. This encapsulates additional information, such as sudden rise or fall in feature values as concepts. Like the setup for tabular dataset, we fix $\mathbf{K} = \mathbf{10}$, i.e. use the top ten features based on logistic regression weights.

We define $\mathbf{K}$ CNNs with two convolutional layers which accept one-dimensional signals as the concept learners for this task. We summarise the results for this task in Table 5. We find that ProbChecklist improves upon the baselines herein as well.

Model	Accuracy	Precision	Recall	Specificity	$\mathbf{d'_k}$	M	T
Logistic Regression	60.627 ± 1.379	0.4887 ± 0.106	0.1843 ± 0.073	0.8792 ± 0.048		-	-
Unit Weighting	60.532 ± 1.567	0.4884 ± 0.087	0.1882 ± 0.102	0.8745 ± 0.066		5 ± 0.63	9.2 ± 0.748
ILP mean thresholds	62.481 ± 0.426	0.529 ± 0.242	0.0529 ± 0.051	0.964 ± 0.031	1	3.4 ± 1.496	3.6 ± 1.85
MIP Checklist	60.767 ± 1.022	0.5117 ± 0.055	0.142 ± 0.05	**0.912 ± 0.036**		3.5 ± 0.866	6.5 ± 1.5
CNN + MLP	63.465 ± 2.048	0.585 ± 0.05	0.234 ± 0.071	0.895 ± 0.021	-		-
CNN + MLP (all features)	**67.19 ± 0.32**	0.526 ± 0.065	0.281 ± 0.041	0.835 ± 0.033		-	-
ProbChecklist	**63.671 ± 1.832**	**0.609 ± 0.115**	**0.354 ± 0.157**	0.823 ± 0.108	3	4.4 ± 1.356	30

Table 5: Performance results for Sepsis Prediction task using Tabular Data.

E.6 SENSITIVITY ANALYSIS

We study the sensitivity of our approach to the number of learnable concepts. In particular, we compare the performance of ProbChecklistwith increasing number of learnt concepts (d'_k). The observed trend for both MNIST (Table 6) and PhysioNet (Table 9) datasets exhibited similarities. We noted a significant improvement in accuracy, precision, and recall when d'_k increased from 1 to 2, suggesting that the samples contain complex features that a single concept cannot represent. Once all the valuable information is captured, accuracy reaches a saturation point and the performance plateaus with d'_k.

$\mathbf{d'_k}$	Evaluation	Accuracy	Precision	Recall	Specificity	T	M
1	Model	86.04 ± 0.463	0.814 ± 0.027	0.412 ± 0.021	0.976 ± 0.004	3	4
	Checklist	72.63 ± 1.42	0.427 ± 0.013	**0.979 ± 0.005**	0.661 ± 0.018		
2	Model	96.888 ± 0.064	0.925 ± 0.008	**0.922 ± 0.012**	0.981 ± 0.003	5	8
	Checklist	92.768 ± 1.6	0.752 ± 0.045	0.97 ± 0.006	0.917 ± 0.02		
3	Model	**97.064 ± 0.187**	0.94 ± 0.008	0.915 ± 0.013	0.985 ± 0.002	7	12
	Checklist	96.52 ± 0.33	0.9 ± 0.009	0.933 ± 0.008	0.973 ± 0.002		
4	Model	97.04 ± 0.177	0.937 ± 0.005	0.917 ± 0.006	0.984 ± 0.001	8.4 ± 1.2	16
	Checklist	**96.808 ± 0.24**	0.917 ± 0.015	0.929 ± 0.01	0.978 ± 0.004		
5	Model	97.032 ± 0.135	**0.943 ± 0.005**	0.91 ± 0.01	**0.986 ± 0.001**	9.4 ± 1.36	20
	Checklist	96.68 ± 0.269	**0.918 ± 0.013**	0.92 ± 0.009	**0.979 ± 0.004**		

Table 6: Performance of ProbChecklist with varying $\mathbf{d'_k}$ on MNIST Checklist Dataset

E.7 CHECKLIST OPTIMIZATION

The checklist generation step from the learnt concepts allows users to tune between sensitivity-specificity depending on the application. The optimal checklist can be obtained by varying the threshold (τ) used to binarize the learnt concepts ($\mathbf{c}_i[j] = \mathbb{I}[\mathbf{p}_i[j] > \tau]$) to optimize the desired metric (Accuracy, F1-Score, AUC-ROC) on the validation data. In Tables 8 and 7, we compare the performance of the checklist obtained by varying the optimization metric.

In the case of the MIMIC mortality prediction task, we also train our models using Binary Cross Entropy (BCE) loss and optimize over the threshold used to binarize the prediction probabilities. Next, we perform a pairwise comparison between the binary cross-entropy loss and ProbChecklist

loss for each optimization metric. From the results in Table 7, it is evident that our method achieves superior performance in terms of accuracy for both metrics.

Loss	Checklist Optimization	Accuracy	Precision	Recall	Specificity	T	M
BCE	Accuracy	76.4±0.6	**0.61±0.03**	0.22±0.09	**0.95±0.02**	-	-
Checklist		**76.61±0.52**	0.59±0.05	**0.24±0.06**	0.94±0.02	6.6±1.74	20
BCE	F1-Score	67.7±3.04	0.41±0.03	**0.62±0.1**	0.7±0.07	-	-
Checklist		**71.45±1.66**	**0.45±0.02**	0.58±0.04	**0.76±0.04**	7.4±1.36	20
Checklist	AUC-ROC	34.49±4.18	0.27±0.01	0.98±0.01	0.13±0.06	4±0	20

Table 7: Results for different Checklist Optimization methods (Accuracy, F1-Score, AUC-ROC) on the MIMIC Mortality Prediction Task for $d'_k = 2$. We report results for the same architecture trained using Binary Cross Entropy (BCE) loss (instead of the proposed ProbChecklist loss) for a fair comparison.

For the PhysioNet Sepsis Prediction Task, we analyze a different aspect of our method. We study the difference in performance by changing the number of learnt concepts per modality (d'_k) for all the metrics.

$\mathbf{d'_k}$	Checklist Optimization	Accuracy	Precision	Recall	Specificity	T	M
1	Accuracy	62.5±1.5	0.67±0.18	0.21±0.13	0.9±0.1	4±0.89	10
	F1-Score	49.22±9.74	0.44±0.06	0.85±0.11	0.27±0.22	3.8±0.98	
	AUC-ROC	40.72±3.72	0.39±0.01	0.93±0.12	0.08±0.13	4±1.22	
2	Accuracy	62.97±3.36	0.58±0.06	0.34±0.18	0.82±0.15	3±1.1	20
	F1-Score	38.98±1.9	0.39±0.02	0.98±0.02	0.01±0.01	2.6±0.8	
	AUC-ROC	48.34±10.56	0.29±0.17	0.54±0.41	0.43±0.43	3.75±1.09	

Table 8: Results for different Checklist Optimization methods (Accuracy, F1-Score, AUC-ROC) on the PhysioNet Sepsis Prediction Task using timeseries. We report results for different values of d'_k.

E.8 Impact of the binarization scheme

In Tables 9 and 6 we show the difference in performance between two types of evaluation schemes. The first scheme is the typical checklist, obtained by binarizing the concept probabilities and thresholding the total number of positive concepts at $\mathbf{T}$. The second is the direct model evaluation, using the non-binarized output probability. It involves only thresholding $\mathbb{P}(\mathbf{d} > \mathbf{T})$ to obtain predictions. As expected, the performance of the checklist is slightly lower than the direct model evaluation because concept weights are binarized leading to a more coarse-grained evaluation.

$\mathbf{d'_k}$	Evaluation	Accuracy	Precision	Recall	Specificity	T	M
1	Model	64.105 ± 1.69	0.586 ± 0.047	0.309 ± 0.025	0.857 ± 0.018	3 ± 0.89	10
	Checklist	63.716 ± 3.02	0.613 ± 0.12	0.233 ± 0.035	0.9 ± 0.036		
2	Model	62.656 ± 2.377	0.525 ± 0.025	0.565 ± 0.032	0.667 ± 0.027	3 ± 1.095	20
	Checklist	62.969 ± 3.355	0.582 ± 0.061	0.343 ± 0.176	0.817 ± 0.145		
3	Model	60.781 ± 2.09	0.503 ± 0.019	0.545 ± 0.026	0.648 ± 0.019	4.4 ± 1.356	30
	Checklist	63.671 ± 1.832	0.609 ± 0.115	0.354 ± 0.157	0.823 ± 0.108		

Table 9: Evaluation of the binarization scheme for sepsis prediction task using time series data.

F Concepts Interpretation

This section provides a detailed analysis of the learnt concepts using TANGOS regularization outlined in Section 4.6.

F.1 TANGOS REGULARIZATION

TANGOS regularization assists in quantifying the contribution of each input dimension to a particular concept. We examine the gradient of each concept obtained from the concept extractors with respect to the input signal. The TANGOS loss consists of two components: The first component enforces sparsity, emphasizing a concentrated subset of the input vector for each concept. The second component promotes uniqueness, minimizing the overlap between the input subsets from which each concept is derived. Sparsity is achieved by taking the L1-norm of the concept gradient attributions with respect to the input vector. To promote decorrelation of signal learned in each concept, the loss is augmented by incorporating the inner product of the gradient attributions for all pairs of concepts.

The degree of interpretability of the concepts can be varied by changing the regularization weights in the TANGOS loss equation 6. For a stronger regularization scheme (i.e. higher regularization weights), the gradient attributions are disentangled and sparse.

$$\mathcal{L}_{TANGOS} = \lambda_{sparsity}\mathcal{L}_{sparsity} + \lambda_{correlation}\mathcal{L}_{correlation} \tag{6}$$

$$= \frac{\lambda_{sparsity}}{N}\sum_{n=1}^{N}\frac{1}{d'_k}\sum_{j=1}^{d'_k}||\frac{\partial p_j(x)}{\partial x_i}||_1 \tag{7}$$

$$+ \frac{\lambda_{correlation}}{N}\sum_{n=1}^{N}\frac{1}{d'_k C_2}\sum_{j=2}^{d'_k}\sum_{l=1}^{d'_k-1}\frac{\langle a^j(x_i), a^l(x_i)\rangle}{||a^j(x_i)||_2, ||a^l(x_i)||_2} \tag{8}$$

where, $a^j(x_i) = \dfrac{\partial p_j(x)}{\partial x_i}$ represents the attribution of j^{th} concept with respect to the i^{th} patient (x_i).

To supplement convergence and enhance the stability of our models, we resort to annealing techniques to gradually increase the weights of these regularization terms.

F.2 MNIST IMAGES

We consider the experimental setup where each encoder learns two concepts per image. Figure 5 shows the gradient attribution heatmaps of Image 2 of the MNIST Dataset with respect to both concepts for four cases. The ground truth concept for this image is **Image 2** $\in \{1, 3, 5, 7, 9\}$.

We observe that there is a significant overlap among the gradient attributions when no regularisation terms were used ($\lambda_{sparsity} = 0$ and $\lambda_{correlation} = 0$), indicating redundancy in the learnt concepts (almost identical representations). However, it manages to identify odd digits correctly and performs well.

For $\lambda_{sparsity} = 10$ and $\lambda_{correlation} = 1$, the concepts correspond to simple features like curvatures and straight lines and are easy to identify. We infer from the gradient heat maps that concepts 1 and 2 focus on the image's upper half and centre region, respectively. Concept 1 is true for digits 5, 8, 9 and 7, indicating that it corresponds to a horizontal line or slight curvature in the upper half. Since Digits 0 and 2 have deeper curvature than the other images, and there is no activity in that region in the case of 4, concept 1 is false for them. concept 2 is true for images with a vertical line, including digits 9, 4, 5 and 7. Therefore, concept 2 is false for the remaining digits (0, 2, 8).

Table 10 highlights the tradeoff between interpretability of the concepts and the checklist performance. By increasing regularization weights, even though checklist accuracy decreases, the gradient attributions disentangle and become sparse. Based on our experiments, the checklist performance is more sensitive to the sparsity weight (i.e. decreases more sharply).

We extend this analysis to the setting with four learnable concepts $d'_k = 4$. Figure 6 ($\lambda_{sparsity} = 10$ and $\lambda_{correlation} = 1$) shows that each concept is focusing on different regions of the image. At least three concepts out of four are true for odd digits, whereas not more than one sample is true for negative samples. This attests to the ability of the method to learn underlying concepts correctly.

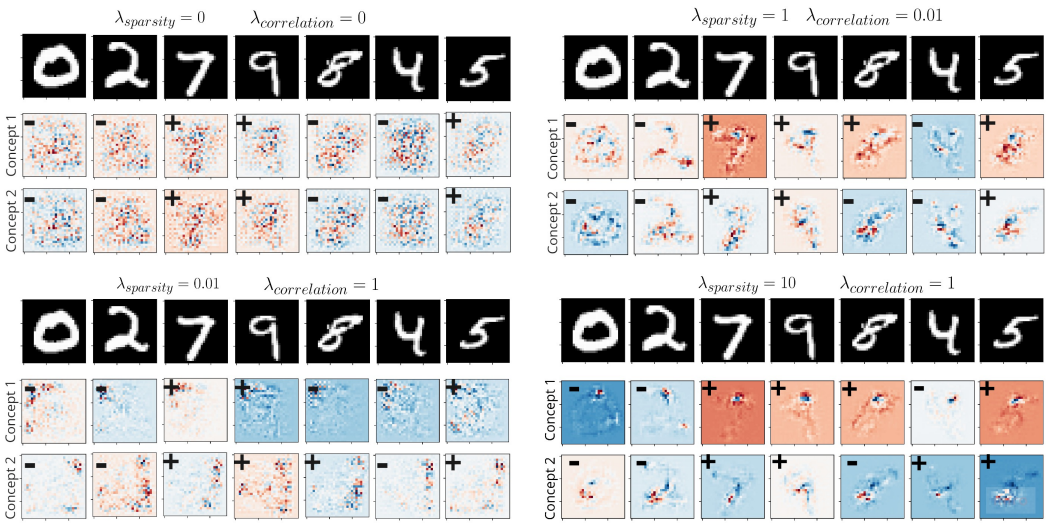

Figure 5: We plot images and corresponding gradient attributions heat maps for seven input samples of the Image 2 modality of the MNIST dataset for different combinations of sparsity and correlation regularization terms. We used a checklist with two learnable concepts per image. The intensity of red denotes the positive contribution of each pixel, whereas blue indicates the negative. If a concept is predicted as true for an image, then we represent that with a plus (+) sign and a negative (-) otherwise.

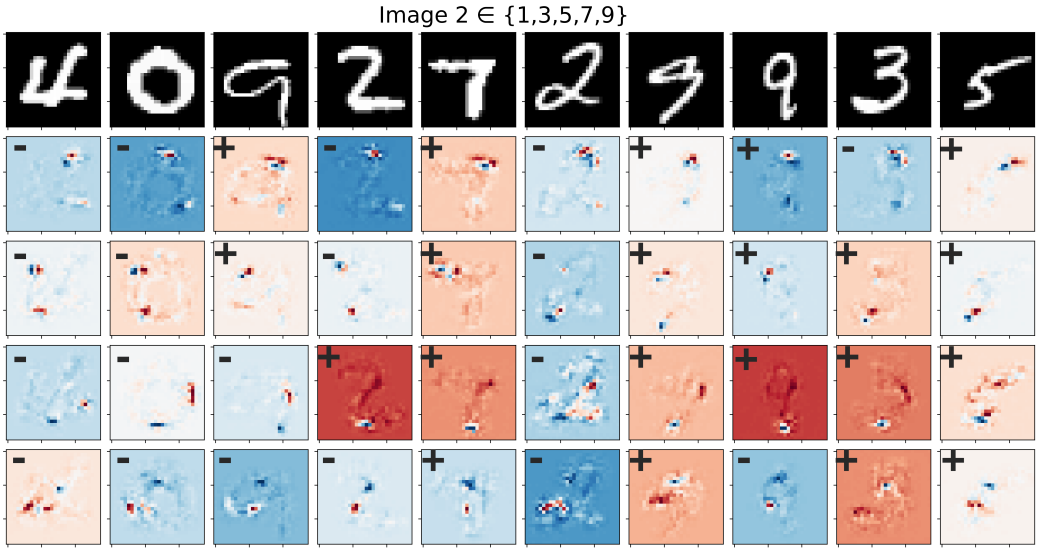

Figure 6: We plot images and corresponding gradient attributions heat maps for seven input samples of the Image 2 modality of the MNIST dataset for $\lambda_{sparsity} = 10$ and $\lambda_{correlation} = 1$. We used a checklist with four learnable concepts per image. The intensity of red denotes the positive contribution of each pixel, whereas blue indicates the negative. If a concept is predicted as true for an image, then we represent that with a plus (+) sign and a negative (-) otherwise.

$\mathbf{d'_k}$	$\lambda_{\mathbf{sparsity}}$	$\lambda_{\mathbf{correlation}}$	**Accuracy**	**Precision**	**Recall**	**Specificity**
2	0	0	95.48	0.829	0.981	0.948
	1	0.01	93.40	0.761	0.988	0.920
	0.01	1	92.88	0.745	0.990	0.913
	10	1	79.28	0.485	0.978	0.733
4	0	0	97.20	0.933	0.930	0.983
	1	0.01	97.04	0.901	0.961	0.973
	0.01	1	96.96	0.904	0.953	0.974
	10	1	78.88	0.491	0.844	0.775

Table 10: Performance of ProbChecklist for different combinations of sparsity ($\lambda_{sparsity}$) and correlation ($\lambda_{correlation}$) regularization weights on MNIST Checklist Dataset

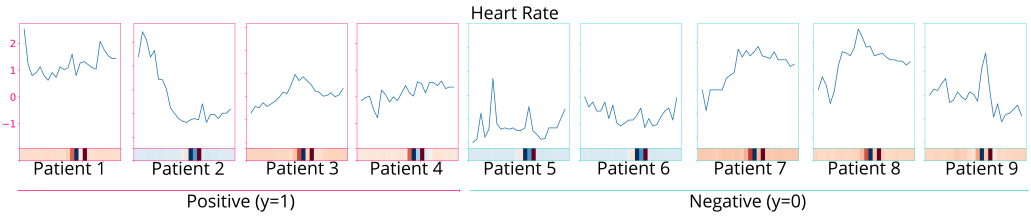

Figure 7: We plot time series for Heart Rate and corresponding gradient attributions for nine patients at $\lambda_{sparsity} = 0.1$ and $\lambda_{correlation} = 10$. The intensity of red denotes the positive contribution of that time step, whereas blue indicates the negative. The border colour of each sample encodes the ground-truth label, with pink being the positive outcome (i.e. mortality).

F.3 MIMIC Time Series

For this analysis, we again fix our training setting to $d'_k = 2$. Sudden changes in slope in the clinical features were associated with switching of the sign gradient attributes. In Figure 7, we plot the time series for heart rate and corresponding gradient attributions for the first concept learnt by CNN. Maximum activity is observed between time steps 12 to 17 for all the patients. If a positive peak (or global maxima) is observed in this period (patients 3, 6, 7, 8), then the gradient at all other time steps has a positive contribution. Another interesting observation is that if the nature of the curve is decreasing and the significant portion has negative values (Images 2, 5, 6), then the surrounding gradient attributions have a negative impact. These features are consistent irrespective of the patient outcome.

From Figure 8, we infer that gradient attributions for both the concepts are identical. In the absence of regularization terms, it was very hard to explain the concepts that were being learnt. Even though interpretability comes at the cost of performance, it helped in mapping learnt concepts to archetypal signals and patterns in the timeseries. Sudden changes in slope in the clinical features were associated with switching of the sign gradient attributes.

With the help of Figure 9, we infer the concepts being learnt when the regularization weights are $\lambda_{sparsity} = 0.1$ and $\lambda_{correlation} = 10$. The region between time steps 11 to 16 is activated for Heart Rate. The learnt concept is negative when there is a sudden increase (peak) in the values around this region as observed in Patients $4, 5, 6, 7$. This concept is true when there is slight fluctuation, or the values are steady around the high gradient region, as seen in the remaining patients. For White Blood Cell Count, our model learns two distinct concepts. The neuron gradient attributions for the first concept are high for time steps 3 to 8. This concept is positive when a local maxima is observed (an increase from the starting value and then a decrease). This pattern is visible in Patients $2, 5$. In all the other cases, a local minima is observed first.

F.4 Medical Abstracts Corpus

Since we only work with text data, we assumed that the concepts learnt are functions of tokens in the text. To obtain interpretable summaries of the concept, we train decision trees on token occurrence

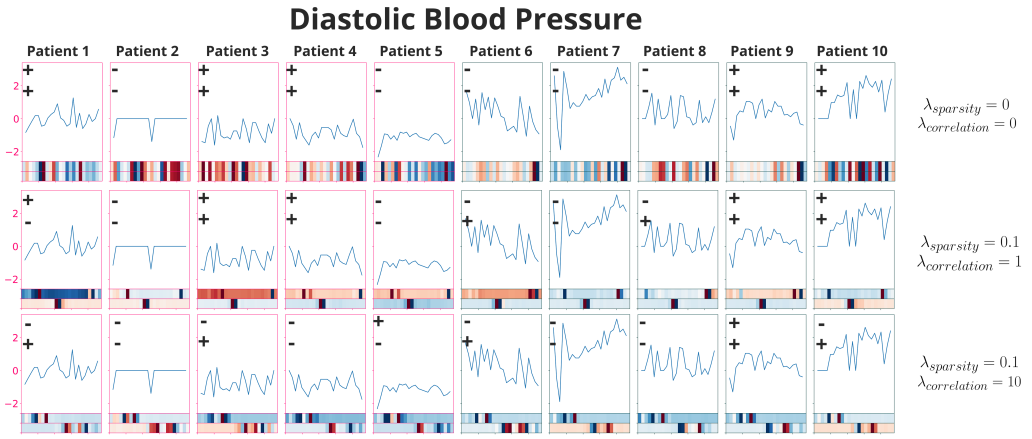

Figure 8: We plot time series for Diastolic Blood Pressure and corresponding gradient attributions for for both concepts for different combinations of regularization weights. The intensity of red denotes the positive contribution of that time step, whereas blue indicates the negative. The border colour of each sample encodes the ground-truth label, with pink being the positive outcome (i.e. mortality). If a concept is predicted as true for a patient, then we represent that with a plus (+) sign and a negative (-) otherwise.

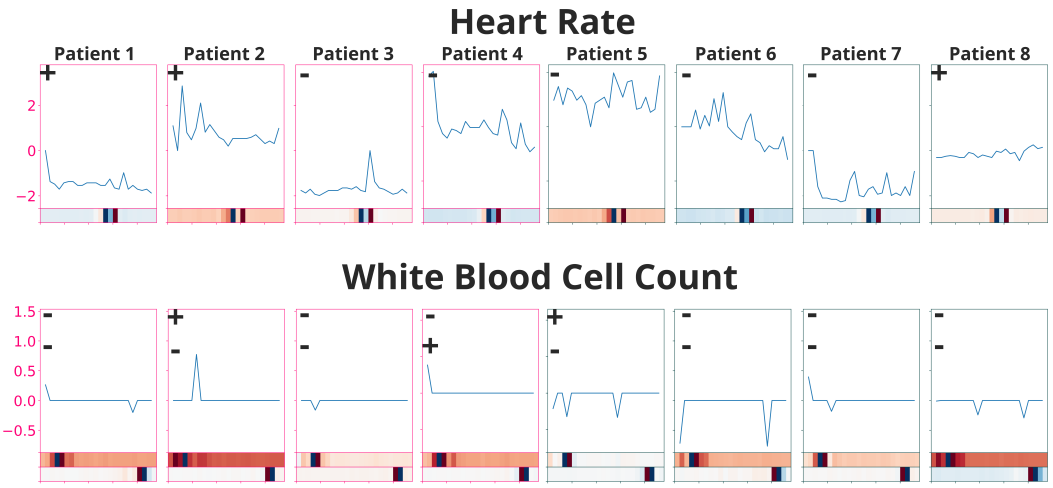

Figure 9: We plot time series for Heart Rate and White Blood Cell Count and corresponding gradient attributions for eight patients for $\lambda_{sparsity} = 0.1$ and $\lambda_{correlation} = 10$. The intensity of red denotes the positive contribution of that time step, whereas blue indicates the negative. The border colour of each sample encodes the ground-truth label, with pink being the positive outcome (i.e. mortality). If a concept is predicted as true for a patient, then we represent that with a plus (+) sign and a negative (-) otherwise.

and use the concept predictions as labels. We then represent each concept by the list of tokens used in the five first layers of each decision tree. We prune this representation by only keeping the unique tokens for each concept.

G Additional Fairness Results

Additionally, we provide FNR and FPR values for each subgroup both before and after applying regularization (Table 11). This is done to ensure that the error rates of majority subgroups, where the performance was originally strong, do not increase. Notably, most minority subgroups benefit from this regularization; however, FNR increases for both the Female (minority) and Male (majority) subgroups after regularization.

Subgroup	Before/After FR	FPR	FNR
Female	Before	0.719	0.0989
	After	0.1899	0.6975
Male	Before	0.4969	0.2931
	After	0.127	0.851
White	Before	0.782	0.937
	After	0.072	0.0868
Black	Before	0.661	0.824
	After	0.0563	0.0597
Others	Before	0.724	0.913
	After	0.064	0.0805

Table 11: We provide the actual values of FNR and FPR for each subgroup before and after fairness regularization is applied.

	Accuracy	Recall	Precision
Without Fairness Regularizer	75.99	0.117	0.648
With Fairness Regularizer	72.412	0.256	0.553

Table 12: We present accuracy, precision, and recall metrics to compare the model's performance before and after applying fairness regularization. Despite observing a decrease in accuracy, the increase in recall signifies a positive development.

H Extension of ProbChecklist: Checklists with learnable integer weights

Checklist structure considers the weight of each item on the checklist as +1. In this section, we propose an extension to allow for integer weights larger than 1 because it has many useful applications and may be of interest to users. Before we formulate a method to learn integer weights for each concept, it is important to note that this would make it harder to interpret the checklist. More specifically, the meaning of the checklist threshold used for classification of samples would now change. Previously, it represented the minimum number of true concepts for a positive classification. Now it signifies a score - the minimum value of the weighted sum of concept probabilities for a positive classification.

Given K data modalities as the input for sample i, we train K concept learners to obtain the vector of probabilistic concepts of each modality $\mathbf{p_i^k} \in [0,1]^{d'_k}$. Next, we concatenate the full concepts probabilities ($\mathbf{p_i}$) for sample i. At this point, we can introduce a trainable weight vector $W \in [0,1]^{d'}$ (with $\sum_{i=1}^{d'} w_i = 1$) of the same dimension as p_i (concept probabilities) which will capture the

relative importance of the features. Element-wise product (◎) of p_i and W represents the weighted concept probabilities and can be denoted with Wp_i. This vector can be normalized by dividing each element with the maximum entry (L0 norm). While training it i For training the concept learners, we pass Wp_i through the probabilistic logic module. After training, the integer weights corresponding to each concept in the checklist can be obtained by converting the W to a percentage: W_{int}. At inference time, we discretize $\mathbf{C_i}$ to construct a complete predictive checklist. Next, compute the score $W_{int}^T C_i$ and compare it against the checklist threshold, M, to classify the sample.

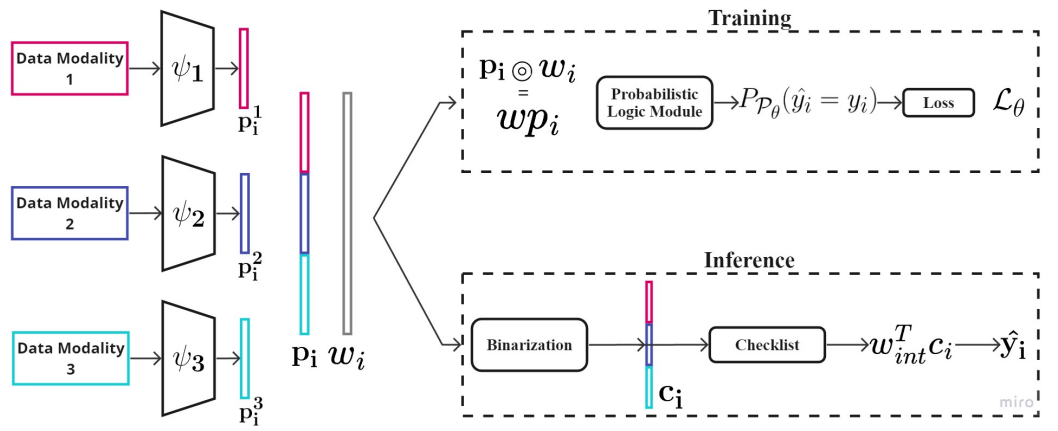

I PLOT: PERFORMANCE RESULTS OF PROBCHECKLIST

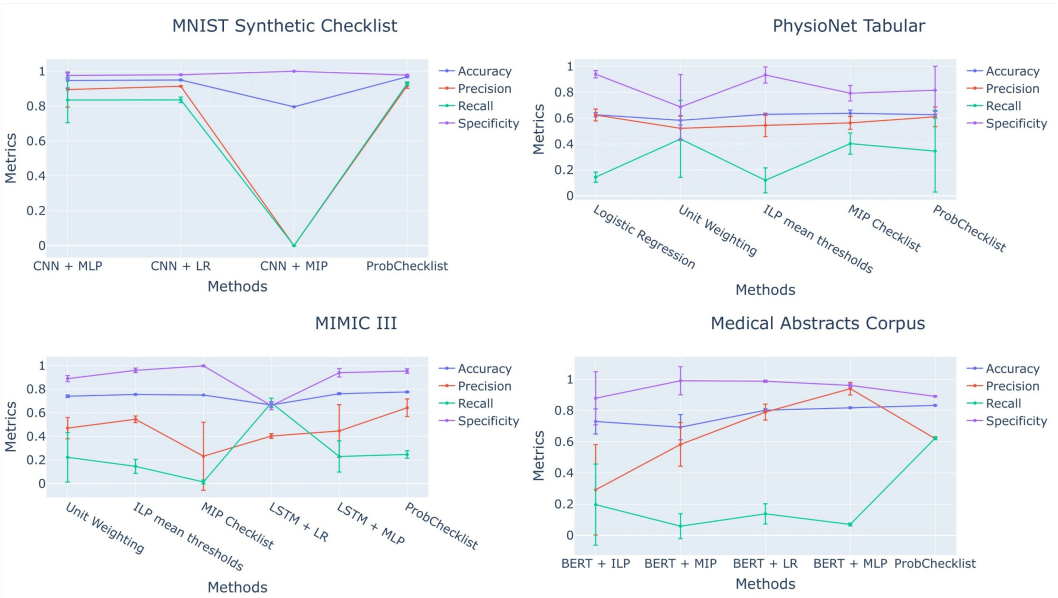

Figure 10: We plot the performance results reported in Table 1.

J IMPLEMENTATION

The code for all the experiments and instructions to reproduce the results are available at `https://anonymous.4open.science/r/ProbChecklist-322A/`. We have extensively used the PyTorch(Paszke et al., 2019) library in our implementations and would like to thank the authors and developers.